Indian Journal of Engineering & Materials Sciences
Vol. 29, April 2022, pp. 181-188

Vibration response of exponentially graded plates on elastic foundation using higher-order shear deformation theory

V Kumar[a*, c], S J Singh[b], V H Saran[c], & S P Harsha[c]

[a]Mechanical Engineering Department, Engineering College, Bikaner, Rajasthan 334 001, India

[b]Department of Mechanical Engineering, Netaji Subhas University of Technology, New Delhi 110 078, India

[c]Vibration and Noise control laboratory, Indian Institute of Technology Roorkee, Uttrakhand 247 667, India

Received: 12 February, 2021; Accepted: 14 February, 2022

A non-polynomial hyperbolic based theory has been presented for the free vibration response of a rectangular plate with linearly varying thickness, which rests on an elastic foundation. Ceramic/ metal has considered as Functionally Graded Material (FGM) of the plate using exponential law for material gradation of properties in the thickness direction. The influence of Winkler's and Pasternak's paremeter of foundation on the plate is investigated in conjunction with taper ratio. The governing equation of plates has established using the variational principle. Galerkin's technique has been followed for the solution of the eigen value problem of the presented model. The obtained results have compared with the observations of the isotropic tapered plate, and FGM plate for uniform thickness. The numerical result depicts the good accuracy of the present theory comparable to the existing shear deformation theory. The influences of thickness variation for a plate, has assumed to be simply supported and clamped, have investigated with various span ratio, aspect ratio, taper ratio and foundation stiffness.

Keywords: Shear deformation plate theory, Two-parameter elastic foundation, Tapered plate, Vibratory response

1 Introduction

FGMs, the advanced composite material, which has received great attention in different engineering application. FGMs have a mixture of materials in which microstructures so tailored to achieve desired properties. These materials have typically made by combining two different materials like ceramic and metal. The advantage of FGM bears on this idea that they can withstand the high-temperature gradient as well as high strength. The ceramic constituents in FGM provide the high-temperature resistance due to bad conductor of heat while metal constituent prevents from the fracture. In 1984, The FGM was first introduce in Japan due to its versatility in various engineering application[1].Thin-walled structures like plates and shells made of FGM have used in reactor vessels, airplane industries, and semiconductor devices, which may be led to failure due to vibratory response. In this regard, the investigation of their dynamic response has quite necessary for the engineering application. Various plate theories have been established in the last two decades to analyze the plate element's behavior.

In this viewpoint, the Classical Plate Theory (CPT) based on the Kirchoff assumption has developed for thin plates without an accounting of transverse shear strains. Free vibration and deformation of isotropic shell based on CPT has been investigated by Love[2]. The small improvement in the First-Order Shear Deformation Theory (FOST) over the CPT, for reasonably thick and thin plates, is to account for the shear deformation effect. Bending, buckling, and modal analysis of FGM plate have been done using FOST [3-5] after selecting the proper Shear Correction Factor (SCF). The selection of suitable SCF in FOST is also a big challenge; to circumvent this condition, Higher-order Shear Deformation Theory (HSDT) comes into the picture, where SCF has not needed. The polynomial and non-polynomial-based HSDT has broadly classified and established for a different type of analysis by the various author[6-10]. Mantri *et al.*[11] has presented a new model based on HSDT in which the stretching effect during static analysis has considered. The variational principle has used to deduce the governing differential equation of motion, and further solution for simply supported plate is obtained using the Navier method.

*Corresponding author (E-mail: vkumar@me.iitr.ac.in)

Furthermore, the plate on an elastic foundation has also been investigated to predict the buckling loads, static and dynamic response of airfield pavement system as well as foundation of buildings, swimming pools, and storage tank. Singh & Harsha[12]have investigated the buckling and vibration effect on sandwich FGM plate resting on Pasternak's foundation, supported with various boundary conditions. Zhou *et al.*[13]have reported the solution for free vibration analysis of a rectangular plate resting on an elastic foundation using three-dimensional elasticity theory.

Malekzadeh [14]has applied the Differential Quadrature method to obtain the vibratory solution of the FG plate on the elastic foundation to be supported with arbitrary boundary conditions. In-order to this, the plate with variable thickness has great importance in real engineering application. Many researcher[15-17] have studied the structural response of isotropic rectangular plate with variable thickness using analytical or numerical methods. Kumar *et al.*[18]have presented the analytical solution of the FGM porous plate resting on Pasternak foundation. Hamilton principle in conjunction with Gelerkin's Vlasov method has applied on variable thick plate supported with various boundary condition.

In the light of above discussion, the static, buckling, and free vibration analysis of tapered isotropic plate have been done by the various researcher. But as per author knowledge, the work on exponential FGM plate with variable thickness resting on two parameter elastic foundation is not reported. So, the current research objective has to investigate the free vibration analysis of the E-FGM (Exponential-Functionally Graded Material)plate having variable thickness on Pasternak exponential FGM (E-FGM) plate which rests on elastic foundation. The two-parameter elastic foundation has been chosen as a Winkler-Pasternak model which works as vertical spring as well as shear layer above the vertical spring.

Moreover, the E-FGM plate material properties are presumed to vary in the direction of thickness according to exponential law of distribution by considering the volume fractions of the constituents. Parametric study based on the various parameter (Span ratio, aspect ratio, taper ratio & foundation stiffness) has carried out to explore the research. Further, some innovative results of E-FGM plate having all the edges have been simply supported as well as clamped have been listed for future perspectives.

2 Materials and Methods

2.1 Exponential-FGM (E-FGM) Plate

A rectangular E-FGM plate of length a and width b, resting on Pasternak foundation is shown in Fig 1. The plate's thickness hywas varying in the y-direction, and the material properties were graded in thickness direction-Z according to exponential distribution law. The material gradation law was considered as given in earlier research[19]. The Young's modulus and density at the top and bottom surface denoted by E_C and E_m.

$$E_{effective}(z) = E_C e^{-\delta\left(1-\frac{2Z}{h_y}\right)},$$

where $,\delta = \frac{1}{2} ln(\frac{E_C}{E_m})$;The following thickness variation parameter was selected in present formulation, where h_1,h_2&$\chi$are the plate thickness and taper ratio (χ).

$$h_y = h_1\left(1+\chi\left(\frac{y}{b}\right)\right)\chi = \frac{h_2-h_1}{h_1}$$

2.2 Problem Formulation

Based on the non-polynomial higher-order shear deformation theory, the displacement field maybe written *from*[20]as,

$$U(x,y,z,t) = u(x,y,t) - z\left(\frac{\partial w}{\partial x}\right) + \left(tanh^{-1}\left(\frac{rz}{h}\right) - z\frac{\frac{r}{h}}{1-\frac{r^2}{4}}\right)\Phi_x(x,y,t)$$

$$V(x,y,z,t) = v(x,y,t) - z\left(\frac{\partial w}{\partial y}\right) + \left(tanh^{-1}\left(\frac{rz}{h}\right) - z\frac{\frac{r}{h}}{1-\frac{r^2}{4}}\right)\Phi_y(x,y,t)$$

$$W(x,y,z,t) = w(x,y,t) \quad ...(1)$$

Here, (u,v,w) denote the displacements of a point on the middle plane, and (Φ_x,Φ_y) denote the rotation about y-axis and x-axis. The shape function $f(Z) = tanh^{-1}\left(\frac{rz}{h}\right) - z\frac{\frac{r}{h}}{1-\frac{r^2}{4}}$was consider with r=0.088. In

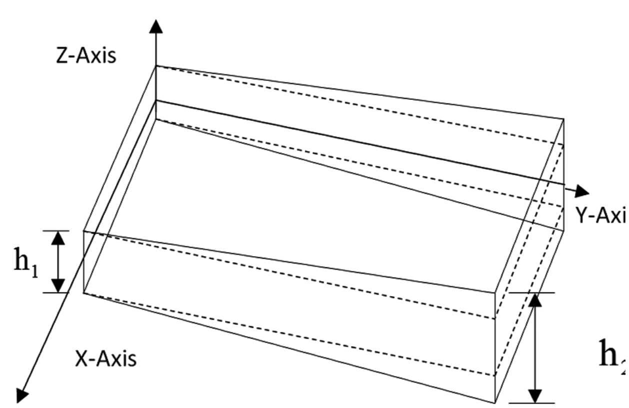

Fig. 1 — Pictorial view of the E-FGM plate having a varying thickness in Y-direction.

short, shape function may write as $f(z) = \lambda(z) + z\vartheta$.The linear strain may be obtained as,

$$\begin{Bmatrix} \varepsilon_{xx} \\ \varepsilon_{yy} \\ \gamma_{yz} \\ \gamma_{xz} \\ \gamma_{xy} \end{Bmatrix} = \begin{Bmatrix} \varepsilon^{(0)}{}_{xx} \\ \varepsilon^{(0)}{}_{yy} \\ 0 \\ 0 \\ \gamma^{(0)}{}_{xy} \end{Bmatrix} + z \begin{Bmatrix} \varepsilon_b{}^{(1)}{}_{xx} \\ \varepsilon_b{}^{(1)}{}_{yy} \\ 0 \\ 0 \\ \gamma_b{}^{(1)}{}_{xy} \end{Bmatrix} + f(z) \begin{Bmatrix} \varepsilon_s{}^{(1)}{}_{xx} \\ \varepsilon_s{}^{(1)}{}_{yy} \\ 0 \\ 0 \\ \gamma_s{}^{(1)}{}_{xy} \end{Bmatrix} + f'(z) \begin{Bmatrix} 0 \\ 0 \\ \gamma^{(0)}{}_{yz} \\ \gamma^{(0)}{}_{xz} \\ 0 \end{Bmatrix} \quad (2)$$

Now the consitutive relation can be established as,

$$\begin{bmatrix} \sigma_{xx} \\ \sigma_{yy} \\ \sigma_{yz} \\ \sigma_{xz} \\ \sigma_{xy} \end{bmatrix} = \begin{bmatrix} C_{11} & C_{12} & 0 & 0 & 0 \\ C_{12} & C_{22} & 0 & 0 & 0 \\ 0 & 0 & C_{44} & 0 & 0 \\ 0 & 0 & 0 & C_{55} & 0 \\ 0 & 0 & 0 & 0 & C_{66} \end{bmatrix} \begin{bmatrix} \epsilon_{xx} \\ \epsilon_{yy} \\ \gamma_{yz} \\ \gamma_{xz} \\ \gamma_{xy} \end{bmatrix}$$

$$C_{11} = C_{22} = \frac{E(z)}{1-\nu^2}, C_{12} = \frac{\nu E(z)}{1-\nu^2} = \frac{\nu E(z)}{1-\nu^2},$$
$$C_{44} = C_{55} = C_{66} = \frac{E(z)}{2(1+\nu)} \quad ...(3)$$

The strain energy relation established as,

$U_P = \frac{1}{2}\int \sigma_{ij}\varepsilon_{ij}dv$, $U_P = \frac{1}{2}\int(\sigma_{xx}\varepsilon_{xx} + \sigma_{yy}\varepsilon_{yy} + \sigma_{xy}\varepsilon_{xy} + \sigma_{yz}\varepsilon_{yz} + \sigma_{zx}\varepsilon_{zx})dv$

Substituting Eqs (2 and 3) in Eq. 4, and after integratingwithrespect to the thickness of the platemay be re-written in variational form as,

$$\delta U_P = \int_A \begin{bmatrix} \left(N_{xx}\delta\varepsilon^{(0)}{}_{xx} + N_{yy}\delta\varepsilon^{(0)}{}_{yy} + N_{xy}\delta\gamma^{(0)}{}_{xy}\right) \\ + \left(M^b{}_{xx}\delta\varepsilon_b{}^{(1)}{}_{xx} + M^b{}_{yy}\delta\varepsilon_b{}^{(1)}{}_{yy} + M^b{}_{xy}\delta\gamma_b{}^{(1)}{}_{xy}\right) + \\ \left(M^s{}_{xx}\delta\varepsilon_s{}^{(1)}{}_{xx} + M^s{}_{yy}\delta\varepsilon_s{}^{(1)}{}_{yy} + M^s{}_{xy}\delta\gamma_s{}^{(1)}{}_{xy}\right) \\ + \left(M^q{}_{xx}\delta\Phi_x + M^q{}_{yy}\delta\Phi_y\right) + \vartheta\left(Q_x\delta\Phi_x + Q_y\delta\Phi_y\right) \end{bmatrix} dxd,$$

$$\begin{Bmatrix} N_{xx} & M^b{}_{xx} & M^s{}_{xx} \\ N_{yy} & M^b{}_{yy} & M^s{}_{yy} \\ N_{xy} & M^b{}_{xy} & M^s{}_{xy} \end{Bmatrix} = \int_{-\frac{h}{2}}^{\frac{h}{2}} (1, z, \lambda(z)) \begin{Bmatrix} \sigma_{xx} \\ \sigma_{yy} \\ \tau_{xy} \end{Bmatrix} dz \begin{Bmatrix} Q_x & M^q{}_{xx} \\ Q_y & M^q{}_{yy} \end{Bmatrix} = \int_{-\frac{h}{2}}^{\frac{h}{2}} (1, \lambda'(z)) \begin{Bmatrix} \tau_{xz} \\ \tau_{yz} \end{Bmatrix} dz \quad ...(5)$$

$$\begin{Bmatrix} N \\ M^b \\ M^s \end{Bmatrix} = \begin{bmatrix} A & B & F \\ B & D & H \\ F & H & J \end{bmatrix} \begin{Bmatrix} \varepsilon \\ \varepsilon_b \\ \varepsilon_s \end{Bmatrix}, \quad ...(6)$$

$$Q = (\vartheta A + K)\gamma_s \quad ...(7)$$

$$Q^q = (\vartheta K + L)\gamma_s \quad ...(8)$$

$$where, \{A_{ij}, B_{ij}, D_{ij}, F_{ij}, H_{ij}, J_{ij}, K_{ij}, L_{ij}\} = \int_{\frac{-h}{2}}^{\frac{h}{2}} C_{ij}\{1, z, z^2, \lambda(z), z\lambda(z), \lambda(z)^2, \lambda'(z), \lambda'(z)^2\} dz$$

The strain energy of the two-parameter elastic foundation in variational form is considered as:

$$\delta U_F = \frac{1}{2}\int (K_w - K_p\nabla^2)\, w\delta w dxdy \quad ...(9)$$

K_w, K_P represents the Winkler, Pasternak foundation stiffness and where $\nabla^2 = \frac{\partial^2}{\partial x^2} + \frac{\partial^2}{\partial y^2}$.

The kinetic energy of the assumed mass system are developed as,

$$\delta T = \frac{1}{2}\int_A \rho(U\delta U + V\delta V + W\delta W)\, dzdA \quad ...(10)$$

After substituting Eq. (1) into Eq. (10), we got,

$$\delta T = \int_A \begin{bmatrix} I_0(u\delta u + v\delta v + w\delta w) - I_1\left(u\frac{\partial\delta w}{\partial x} + \frac{\partial w}{\partial x}\delta u + v\frac{\partial\delta w}{\partial y} + \frac{\partial w}{\partial y}\delta v\right) + \\ I_2\left(\frac{\partial w}{\partial x}\frac{\partial\delta w}{\partial x} + \frac{\partial w}{\partial y}\frac{\partial\delta w}{\partial y}\right) + J_1(u\delta\emptyset_x + \emptyset_x\delta u + v\delta\emptyset_y + \emptyset_y\delta v) - J_2 \\ \left(\frac{\partial w}{\partial x}\delta\emptyset_x + \emptyset_x\frac{\partial\delta w}{\partial x} + \frac{\partial w}{\partial y}\delta\emptyset_y + \emptyset_y\frac{\partial\delta w}{\partial y}\right) \end{bmatrix} dxdy \quad ...(11)$$

where, $\{I_0, I_1, I_2, J_1, J_2, J_3\} = \int_{-\frac{h}{2}}^{\frac{h}{2}} \rho\{1, z, z^2, f(z), zf(z), f(z)^2\} dz$

Hamilton's principle was used here to obtain the equation of motion, and analyticallyrepresented as,

$$\int_{t_1}^{t_2} (\delta U_P + \delta U_F - \delta T)\, dt = 0 \quad ...(12)$$

Putting Eqs (5, 9, and 11) into Eq.12 and collecting the coefficient of $\delta u, \delta v, \delta w, \Phi_x \& \Phi_y$, we got the equation of motion for the plate,

$$\delta u: \frac{\partial N_{xx}}{\partial x} + \frac{\partial N_{xy}}{\partial y} = I_0 u - I_1\frac{\partial w}{\partial x} + J_1\Phi_x$$
$$\delta v: \frac{\partial N_{yy}}{\partial y} + \frac{\partial N_{xy}}{\partial x} = I_0 v - I_1\frac{\partial w}{\partial y} + J_1\Phi_y$$
$$\delta w: \left(\frac{\partial^2 M^b{}_{xx}}{\partial x^2} + \frac{\partial^2 M^b{}_{yy}}{\partial y^2} + 2\frac{\partial^2 M^b{}_{xy}}{\partial x\partial y}\right) = U_F + I_0 w + I_1\left(\frac{\partial u}{\partial x} + \frac{\partial v}{\partial y}\right) - I_2\nabla^2 w + J_2\left(\frac{\partial\Phi_x}{\partial x} + \frac{\partial\Phi_y}{\partial y}\right)$$
$$\delta\Phi_x: \frac{\partial M^s{}_{xx}}{\partial x} + \vartheta\frac{\partial M^b{}_{xx}}{\partial x} + \frac{\partial M^s{}_{xy}}{\partial y} + \vartheta\frac{\partial M^b{}_{xy}}{\partial y} - M^q{}_{xx} - \vartheta Q_x = J_1 u - J_2\frac{\partial w}{\partial x} + J_3\Phi_x$$
$$\delta\Phi_y: \frac{\partial M^s{}_{yy}}{\partial y} + \vartheta\frac{\partial M^b{}_{yy}}{\partial y} + \frac{\partial M^s{}_{xy}}{\partial x} + \vartheta\frac{\partial M^b{}_{xy}}{\partial x} - M^q{}_{yy} - \vartheta Q_y = J_1 v - J_2\frac{\partial w}{\partial y} + J_3\Phi_y \quad ...(13)$$

Substitute A_{ij}, B_{ij}, D_{ij} ….. into Eq.(13), and rewrite in simplyfied form where $R_{ij}$is linear operator, discussed in **Appendix A**.

$$R_{11}u + R_{12}v - R_{13}w + R_{14}\Phi_x + R_{15}\Phi_y = I_0 u - I_1\frac{\partial w}{\partial x} + J_1\Phi_x$$
$$R_{21}u + R_{22}v - R_{23}w + R_{24}\Phi_x + R_{25}\Phi_y = I_0 v - I_1\frac{\partial w}{\partial y} + J_1\Phi_y$$
$$R_{31}u + R_{32}v - R_{33}w + R_{34}\Phi_x + R_{35}\Phi_y - U_F = I_0\bar{w} + I_1\left(\frac{\partial u}{\partial x} + \frac{\partial v}{\partial y}\right) - I_2\nabla^2 w + J_2\left(\frac{\partial\Phi_x}{\partial x} + \frac{\partial\Phi_y}{\partial y}\right)$$
$$R_{41}u + R_{42}v - R_{43}w + R_{44}\Phi_x + R_{45}\Phi_y = J_1 u - J_2\frac{\partial w}{\partial x} + J_3\Phi_x$$
$$R_{51}u + R_{52}v - R_{53}w + R_{54}\Phi_x + R_{55}\Phi_y = J_1 v - J_2\frac{\partial w}{\partial y} + J_3\Phi_y \quad 14$$

2.3 Methodology

Considering a simply supported rectangular plate having variable thickness on Pasernak foundation, with boundary conditions used in the present theory.

$v = w = \Phi_x = N_{xx} = M_{xx}^b = M_{xx}^S = 0$, on edge x=(0,a)
$u = w = \Phi_y = N_{yy} = M_{yy}^b = M_{yy}^S = 0$, on edge y=(0,b)

The Galerkin method was adopted to find the solution of the differential equation of motion. The following shape function, for free vibration analysis, was applied in the present formulation.

$$\{u(x,y), \Phi_x(x,y)\} = \sum_{m=1}^{\infty}\sum_{n=1}^{\infty}\{U^{mn}, {\theta_x}^{mn}\}\frac{\partial X_m(x)}{\partial x} Y_n(y)e^{i\omega t}$$

$$\{v(x,y), \Phi_y(x,y)\} = \sum_{m=1}^{\infty}\sum_{n=1}^{\infty}\{V^{mn}, {\theta_y}^{mn}\} X_m(x)\frac{\partial Y_n(y)}{\partial y} e^{i\omega t} \quad 15$$

$$w(x,y) = \sum_{m=1}^{\infty}\sum_{n=1}^{\infty} W^{mn} X_m(x) Y_n(x) e^{i\omega t}$$

where, $U^{mn}, V^{mn}, W^{mn}, {\theta_x}^{mn}, {\theta_y}^{mn}$ were the unknown parameters and ω denotes the eigen frequency associated with (m, n)th mode shape. The suggested function X_m (x)&Y_n (y) should satisfy the geometric boundary condition for simply supported plate. The shape function were assumed as,

$X_m(x) = sin(\alpha x), Y_n(y) = sin(\beta y)$,

where, $\alpha = \frac{m\pi}{a}, \beta = \frac{n\pi}{b}$

On putting Eq. (15) into the governing Eq. (14) and multiplying them by the corresponding eigen function. After integrating the domain of solution and some mathematical manipulations, the following algebraic equations were obtained.

$$\kappa_{ij} = \begin{bmatrix} \kappa_{11} & \kappa_{12} & \kappa_{13} & \kappa_{14} & \kappa_{15} \\ \kappa_{21} & \kappa_{22} & \kappa_{23} & \kappa_{24} & \kappa_{25} \\ \kappa_{31} & \kappa_{32} & \kappa_{33} & \kappa_{34} & \kappa_{35} \\ \kappa_{41} & \kappa_{42} & \kappa_{43} & \kappa_{44} & \kappa_{45} \\ \kappa_{51} & \kappa_{52} & \kappa_{53} & \kappa_{54} & \kappa_{55} \end{bmatrix},$$

$$M_{ij} = \begin{bmatrix} -I_0\mu_6 & 0 & I_1\mu_6 & -J_1\mu_6 & 0 \\ 0 & -I_0\mu_2 & I_1\mu_2 & 0 & -J_1\mu_2 \\ -I_1\mu_9 & -I_1\mu_3 & -I_0\mu_1 + I_2(\mu_3+\mu_9) & -J_2\mu_9 & -J_2\mu_3 \\ -J_1\mu_6 & 0 & J_2\mu_6 & -J_3\mu_6 & 0 \\ 0 & -J_1\mu_2 & J_2\mu_2 & 0 & -J_3\mu_2 \end{bmatrix}$$

In which,

$$\kappa_{11} = \int_0^a\int_0^b (A_{11}\mu_{12} + A_{66}\mu_8)\,dxdy$$

$$\kappa_{12} = \int_0^a\int_0^b ((A_{12} + A_{66})\mu_8)\,dxdy$$

$$\kappa_{13} = -\int_0^a\int_0^b (B_{11}\mu_{12} + (B_{12} + 2B_{66})\mu_8)\,dxdy$$

$$\kappa_{14} = \int_0^a\int_0^b ((\vartheta B_{11} + F_{11})\mu_{12} + (\vartheta B_{66} + F_{66})\mu_8)\,dxdy$$

$$\kappa_{15} = \int_0^a\int_0^b \mu_8\big(\vartheta(B_{12} + B_{66}) + (F_{12} + F_{66})\big)\,dxdy$$

$$\kappa_{31} = \int_0^a\int_0^b (B_{11}\mu_{13} + (B_{12} + 2B_{66})\mu_{11})\,dxdy$$

$$\kappa_{32} = \int_0^a\int_0^b (B_{22}\mu_5 + (B_{12} + 2B_{66})\mu_{11})\,dxdy$$

$$\kappa_{33} = -\int_0^a\int_0^b (D_{11}\mu_{13} + (2D_{12} + 4D_{66})\mu_{11} + D_{22}\mu_5 + K_w\mu_1 - K_P(\mu_3 + \mu_9))\,dxdy$$

$\kappa_{34} = \int_0^a\int_0^b \Big(\mu_{13}(H_{11} + \vartheta D_{11}) + \mu_{11}\big((H_{12} + 2H_{66}) + \vartheta(D_{12} + 2D_{66})\big)\Big)\,dxdy$ $\kappa_{35} = \int_0^a\int_0^b \Big(\mu_5(H_{22} + \vartheta D_{22}) + \mu_{11}\big((H_{12} + 2H_{66}) + \vartheta(D_{12} + 2D_{66})\big)\Big)\,dxdy$

$$\kappa_{51} = \int_0^a\int_0^b \mu_{10}\big(\vartheta(B_{12} + B_{66}) + (F_{12} + F_{66})\big)\,dxdy$$

$$\kappa_{52} = \int_0^a\int_0^b \mu_{10}(\vartheta B_{66} + F_{66}) + \mu_4(\vartheta B_{22} + F_{22})\,dxdy$$

$\kappa_{53} = -\int_0^a\int_0^b \Big(\mu_4(H_{22} + \vartheta D_{22}) + \mu_{10}\big((H_{12} + 2H_{66}) +$ $\vartheta D12+2D66dxdy$

$\kappa_{54} = \int_0^a\int_0^b \mu_{10}\big(\vartheta(\vartheta D_{12} + H_{12}) + (J_{12} + \vartheta H_{12}) + \vartheta(\vartheta D_{66} +$ $H66+J66+\vartheta H66dxdy$

$\kappa_{55} = \int_0^a\int_0^b (\vartheta^2 D_{22} + 2\vartheta H_{22} + J_{22})\mu_4 + (\vartheta^2 D_{66} + 2\vartheta H_{66} +$ $J66\mu10-\vartheta2A44+2\vartheta K44+L44\mu2dxdy$

$\{\mu_1, \mu_3, \mu_5, \mu_7, \mu_9, \mu_{11}, \mu_{13}\} = \{X_m Y_n, X_m {Y_n}'', X_m {Y_n}^{iv}, {X_m}' {Y_n}', {X_m}'' Y_n, {X_m}'' {Y_n}'', {X_m}^{iv} Y_n\} X_m Y_n$
$\{\mu_2, \mu_4, \mu_{10}\} = \{X_m {Y_n}', X_m {Y_n}''', {X_m}'' {Y_n}'\} X_m {Y_n}'$,
$\{\mu_6, \mu_8, \mu_{12}\} = \{{X_m}' X_n, {X_m}' {Y_n}'', {X_m}''' Y_n\} {X_m}' Y_n$

3 Results and Discussion

The ceramic/metal rectangular plate had been considered which rests on the two-parameter elastic foundation for free vibration analysis and discussed some numerical examples for establishing the accuracy of the present formulation. The Al/Al_2O_3 plate was considered all over the study, otherwise specified the FG material during the investigation. The FG materials consist of alumina and aluminum with the following properties,

- Metal (Aluminum, Al): E_m=70 GPa,; Poison ratio=0.3; Density= 2702 Kg/m^3
- Ceramic (Alumina, Al_2O_3): E_C=380 GPa; Poison ratio=0.3; Density= 3800 Kg/m^3
- Ceramic (Alumina, ZrO_2): E_C=151 GPa; Poison ratio=0.3; Density= 3000 Kg/m^3

The following non-dimensional parameters of frequency and foundation stiffness are applied during the investigation.

$$Frequency = \omega\frac{a^2}{h}\sqrt{\rho_C/E_C}\ , \overline{K}_w = \frac{K_w b^4}{D_n}, \overline{K_P \frac{K_P b^2}{D_n}}, D_n = \frac{E_m h^3}{12(1-\nu^2)}$$

In addition, a first numerical example for the vibratory response of a taper isotropic plate had taken to validate the present formulation for the taper plate. The current results are compared with the results obtained by Mizusawa[21]applyingthespline strip method in conjunction with FOSD theory. The isotopic plate was divided into a small-small strip to investigate the free vibration response, and all the edges were simply supported. The results mentioned in Table 1 werein agreement with the result obtained by Mizusawa[21]. The small error may be present due to the (a) adoption of shear deformation theory, as present formulation is based on higher order shear deformation theory (b) Present method was based on analytical approach while published result calculated by numerical technique. As there is no need of Shear Correction Factor (SCF) while in FOST needed SCF. The non-dimensional frequency parameter in comparing results was assumed as mentioned above.

Table 1 — Frequency parameter variation of tapered rectangular plate for different span ratio, tapered ratio and aspect ratio

b/h	χ	a/b	Non-dimensional Frequency	
			Present	Ref.[21]
100	0.25	0.5	13.803	13.817
		1.0	22.130	22.164
		2.0	55.353	55.368
	0.50	0.5	15.191	15.230
		1.0	24.429	24.543
		2.0	61.144	61.185
	0.75	0.5	16.529	16.590
		1.0	26.666	26.880
		2.0	66.792	66.837
10	0.25	0.5	12.512	12.506
		1.0	21.213	21.223
		2.0	53.886	53.853
	0.50	0.5	13.541	13.537
		1.0	23.237	23.281
		2.0	59.263	59.140
	0.75	0.5	14.492	14.479
		1.0	25.177	25.243
		2.0	64.484	64.167

The second example was presented here for validating the accuracy of exponential graded material plate for uniform thickness, as results for E-FGM tapered plate were not available as per author knowledge. The free vibration response of rectangular E-FGM plate was investigated using Classical plate theory by Chakraverty & Pradhan[19]. The governing equation of motion were solved by applying the Rayleigh-Ritz method after adopting the harmonic algebraic displacement function. In order to this, the E-FGM plate's vibration response was compared in Table 2 for simply supported and clamped plate. The outcomes of the comparable results shown a good agreement with published works.

After validation of the current formulation for free vibration of rectangular plates through comparison studies with taking two examples, the effect of the elastic foundation on exponential FG plate for variable thickness is examined, for the first time. For accomplished this, the non-dimensional frequency of the isotropic (Ceramic) and FG material plate was considered with a two-parameter elastic foundation ($\overline{K}_W$, $\overline{K}_P$=50,50), tabulated in Table 3. The taper ratio for the plate was selected as χ=0.10,.25,0.50, 0.75 & 1.0 with span ratio b/h=10. Examining tabulated results reveals that non-dimensional frequencies of the ceramic plate was more than the FG materials plate at each and every taper ratio. It is quite obvious, the stiffness of the ceramic material was always more than the FG material, as the FGM was a mixture of two materials, which reduces the stiffness of the plate. Results in Table 4 and Table 5 are tabulated for E-FGM tapered plate with two different span ratio (b/h=10, 100). Tabulated results in Table 4, were considered for simply supported plate, reveal that the non-dimensional frequency was continuously increasing when the taper and aspect ratio increases. A similar type of trend was found in Table 5, where

Table 2 — Comparison of E-FGM uniform thick plate for free vibration, supported with SSSS & CCCC boundary conditions

a/b	SSSS		CCCC	
	Present	Ref.[19]	Present	Ref.[19]
0.5	8.03420	8.1895	14.6308	16.316
1.0	13.4463	13.103	23.9817	23.890
2.0	34.0274	32.758	66.0194	65.265

Table 3 — Variation of frequency of Ceramic and E-FGM square plate, having span ratio b/h=10 and elastic stiffness ($\overline{K}_W$, $\overline{K}_P$=50,50)

χ	SSSS		CCCC	
	Ceramic	E-FGM	Ceramic	E-FGM
0.10	24.5901	21.013	38.8617	30.5629
0.25	26.187	22.3896	41.2878	32.5341
0.50	28.7352	24.5825	45.2754	35.7959
0.75	31.1818	26.6861	49.1738	39.0135
1.00	33.5572	28.7288	52.9700	42.1770

Table 4 — Frequency parameter for E-FGM plate having various taper ratio (χ=0.25,0.50,0.75& 1.0) with different aspect ratio (a/b=0.5, 1.0) of SSSS boundary conditions

b/h	$\overline{K}_W$	$\overline{K}_P$	a/b=0.50				a/b=1.0			
			χ=0.25	χ=0.5	χ=0.75	χ=1.0	χ=0.25	χ=0.5	χ=0.75	χ=1.0
10	0	0	8.8454	9.5772	17.7556	19.0751	14.963	16.3904	17.7556	19.0751
	100	0	8.9369	9.6784	18.8037	20.2100	15.8319	17.3504	18.8037	20.2100
	0	100	12.5903	13.7038	32.7063	35.2230	27.4186	30.1172	33.2791	35.2229
	100	100	12.6545	30.6461	33.2791	35.8384	27.9009	30.6460	33.2791	35.8383
100	0	0	9.7216	10.6980	11.6384	20.2973	15.585	17.1971	18.762	20.2973
	100	0	9.8085	10.7929	11.7409	21.4010	16.4377	18.1360	19.784	21.4010
	0	100	13.3528	14.6735	15.9415	36.3148	27.9594	30.8230	33.5953	36.3148
	100	100	13.416	14.7422	16.0154	36.9333	28.4425	31.3531	34.1702	36.9333

Table 5 — Frequency parameter for E-FGM plate having various taper ratio (χ=0.25,0.50,0.75& 1.0) with different aspect ratio (a/b=0.5, 1.0) of CCCC boundary conditions

b/h	$\overline{K}_W$	$\overline{K}_P$	a/b=0.50				a/b=1.0			
			χ=0.25	χ=0.5	χ=0.75	χ=1.0	χ=0.25	χ=0.5	χ=0.75	χ=1.0
10	0	0	15.8672	17.0303	18.1139	19.1178	26.5375	29.0287	31.4414	33.7683
	100	0	15.9196	17.0908	18.1832	19.1963	27.0416	29.5996	32.0822	34.4819
	0	100	18.9535	20.5748	22.1467	23.6669	37.2056	41.0451	44.8599	48.6375
	100	100	18.9974	20.6249	22.2033	23.7303	37.5669	41.451	45.3116	49.1361
100	0	0	19.8814	22.1584	24.4662	26.793	29.1266	32.4442	35.8014	39.1875
	100	0	19.9248	22.2068	24.5197	26.8516	29.5966	32.9688	36.3816	39.824
	0	100	22.5084	25.0903	27.7084	30.3492	39.3354	43.8322	48.3884	52.9878
	100	100	22.5467	25.133	27.7556	30.401	39.6847	44.2221	48.8195	53.4607

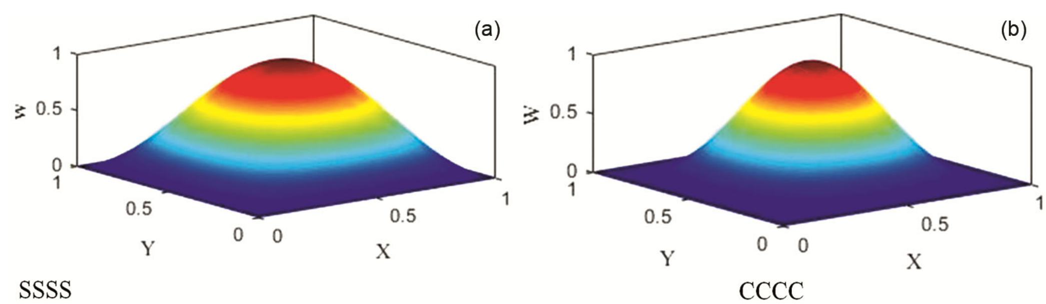

Fig. 2 — Pictorial representation of the plate's first mode shape when all the edges are (a) simply supported, and (b) clamped-clamped.

all the plate edges were fully clamped. For both the span ratio and boundary conditions, one thing was common, the effect of Pasternak's foundation was more significant than the Winkler's foundation. When, we applied the shear layer above the Winkler's foundation, the frequency increases rapidly. The pictorial representation shown in Fig. 2 are for the free vibration analysis. The first mode shape (m, n =1,1) was for the plate, where all the edges are simply supported and clamped.

Comparative results for non-dimensional frequency parameter of SSSS & CCCC edge plate with various taper ratios had been listed in Table 6. Here, the elastic stiffness ($\overline{K}_W$, $\overline{K}_P$=50,50) was taking constant with various span ratio (b/h=10,20,50,80,100) during the investigation. The outcomes after examining the results, the frequency parameter increases on the increase of boundary constraints.

Figure 3 depicts the results of rectangular plate for vibration analysis having taper ratio 0.25, and foundation stiffness($\overline{K}_W$, $\overline{K}_P$=50,50). The results have compared for isotropic (ceramic) and E-FGM (Al/ ZrO_2) plate with two different boundary conditions by changing the span ratio from 1.5 to 2.0. The common observation from the plots are observed that the frequency increases on increase of span ratio. The frequency for ceramic plate was always more than the Al/ZrO_2 plate as well as in case of clamed boundary conditions.

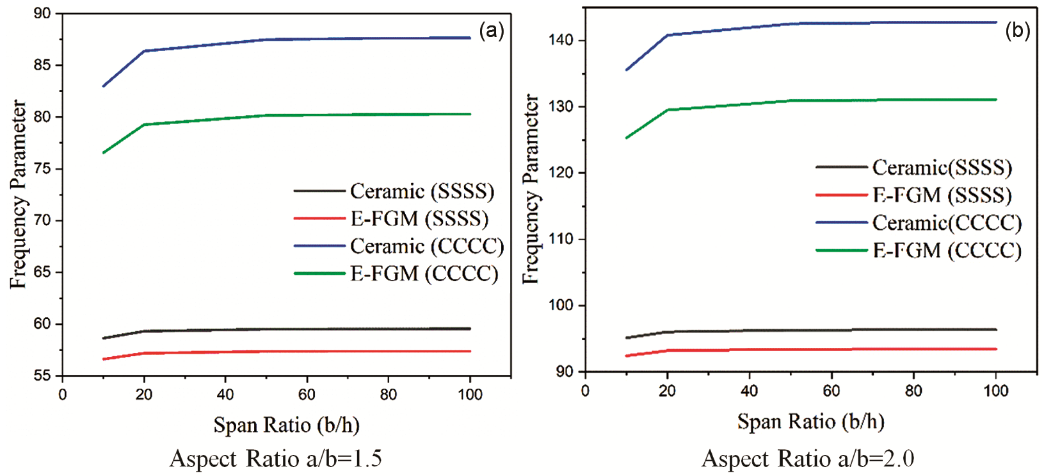

Fig. 3 — Variation of frequency with respect to span ratio for SSSS, and CCCC boundary conditions.

Table 6 — Comparative study of frequency parameter for simply supported & clamped edge, square E-FGM plate with different span ratio, taper ratio and, elastic stiffness ($\overline{K}_W$,$\overline{K}_P$=50,50)

b/h	SSSS				CCCC			
	χ=.25	χ=0.5	χ=0.75	χ=1.0	χ=0.25	χ=0.5	χ=0.75	χ=1.0
10	22.3896	24.5825	26.6861	28.7288	32.5341	35.7959	39.0135	42.177
20	22.7933	25.1056	27.3394	29.5242	34.1833	37.9379	41.7035	45.4643
50	22.9171	25.2686	27.5463	29.7801	34.7358	38.6815	42.6717	46.6926
80	22.9318	25.288	27.5711	29.8109	34.8031	38.773	42.7924	46.8475
100	22.9352	25.2925	27.5769	29.818	34.8187	38.7942	42.8205	46.8837

4 Conclusion

The foregoing research has shown how semi-analytical solution methods can be pursued to obtain a variety of exciting and valuable results for the E-FGM plate's vibratory response, being the linearly varying thickness with a possible combination of boundary conditions. This procedure has employed in a variety of plates as thin to thick plates, by changing the span ratio and square to a rectangular plate by changing the aspect ratio. It has found that on the increase of taper and aspect ratio, frequency increases significantly. Also, the increase in edge constraints leads a significant increase in frequency parameters. One more important observation regarding elastic foundation, the influence of the Pasternak's foundation has more substantial than the Winkler's foundation.

Appendix A

$R_{11} = A_{11}\frac{\partial^2}{\partial x^2} + A_{66}\frac{\partial^2}{\partial y^2}$; $R_{12} = (A_{12} + A_{66})\frac{\partial^2}{\partial x \partial y}$; $R_{13} = B_{11}\frac{\partial^3}{\partial x^3} + (B_{12} + 2B_{66})\frac{\partial^3}{\partial x \partial y^2}$ $R_{14} = (\vartheta B_{11} + F_{11})\frac{\partial^2}{\partial x^2} + (\vartheta B_{66} + F_{66})\frac{\partial^2}{\partial y^2}$; $R_{15} = \left(\vartheta(B_{12} + B_{66}) + (F_{12} + F_{66})\right)\frac{\partial^2}{\partial x \partial y}$

$R_{22} = A_{22}\frac{\partial^2}{\partial y^2} + A_{66}\frac{\partial^2}{\partial x^2}$; $R_{23} = B_{22}\frac{\partial^3}{\partial y^3} + (B_{12} + 2B_{66})\frac{\partial^3}{\partial x^2 \partial y}$; $R_{24} = (\vartheta(B_{12} + B_{66}) + F_{12} + F_{66})\frac{\partial^2}{\partial x \partial y}$ $R_{25} = (\vartheta B_{66} + F_{66})\frac{\partial^2}{\partial x^2} + (\vartheta B_{22} + F_{22})\frac{\partial^2}{\partial y^2}$; $R_{33} = D_{11}\frac{\partial^4}{\partial x^4} + D_{22}\frac{\partial^4}{\partial y^4} + 2(D_{12} + 2D_{66})\frac{\partial^4}{\partial x^2 \partial y^2}$ $R_{34} = (\vartheta D_{11} + H_{11})\frac{\partial^3}{\partial x^3} + (H_{12} + \vartheta(D_{12} + 2D_{66}) + 2H_{66})\frac{\partial^3}{\partial x \partial y^2}$ $R_{35} = (\vartheta D_{22} + H_{22})\frac{\partial^3}{\partial y^3} + (H_{12} + \vartheta(D_{12} + 2D_{66}) + 2H_{66})\frac{\partial^3}{\partial x^2 \partial y}$

$R_{44} = \left(\vartheta(H_{11} + \vartheta D_{11}) + (J_{11} + \vartheta H_{11})\right)\frac{\partial^2}{\partial x^2} + \left(\vartheta(H_{66} + \vartheta D_{66}) + (J_{66} + \vartheta H_{66})\right)\frac{\partial^2}{\partial y^2} - (L_{55} + \vartheta^2 A_{55} + 2\vartheta K_{55})$ $R_{45} = \left(\vartheta(H_{12} + \vartheta D_{12}) + (J_{12} + \vartheta H_{12}) + \vartheta(H_{66} + \vartheta D_{66}) + (J_{66} + \vartheta H_{66})\right)\frac{\partial^2}{\partial x \partial y}$ $R_{55} = \left(\vartheta(H_{66} + \vartheta D_{66}) + (J_{66} + \vartheta H_{66})\right)\frac{\partial^2}{\partial x^2} + \left(\vartheta(H_{22} + \vartheta D_{22}) + (J_{22} + \vartheta H_{22})\right)\frac{\partial^2}{\partial y^2} - (L_{44} + \vartheta^2 A_{44} + 2\vartheta K_{44})\Phi_y$

Reference

1 Koizumi M: *Compos Part B Eng,* 28(1997)1.
2 Love A E H: *Phil, Trans Roy Soc,*179 (1888) 491.
3 Hosseini-Hashemi S, Rokni Damavandi Taher,H, Akhavan H, Omidi M, Thai H T, & Choi D H, *Appl MathModel,* 101 (2010) 1276.
4 Thai H T, & Choi D H: *Compos Part B Eng,* 43 (2012) 2335.
5 Akhavan H, Hashemi S H, Taher H R D, Alibeigloo A, & Vahabi S, *Comput Mater Sci,* 44 (2009) 951.
6 Singh S J, & Harsha S P: *J Vib Eng Technol,*(2018) 67.

7 Singh S J, & Harsha S P:*Thin-Walled Struct,* 150 (2020) 106668.

8 Kumar V, Singh S J, Saran, V H, & Harsha S P, *Mater Today Proc,* 28 (2020) 1719.

9 Reddy J N:*Int J Numer Meth Engng,* 47 (2000) 663.

10 Kumar V, Singh S J, Saran V H, & Harsha S P, *Proc Inst Mech Eng Part L J Mater Des Appl,* 235 (2020) 880.

11 Mantari J L, Guedes Soares, C: *Compos Part B Eng,* 45 (2013) 268.

12 Singh S J, & Harsha S P: *Int J Struct Stab Dyn,* 19 (2019) 1950028.

13 Zhou D, Cheung, Y K Lo, S H Au, F T K, *Int J Numer Methods Eng*, 59 (2004) 1313.

14 Malekzadeh P: *Compos Struct*, 89 (2009) 367.

15 T Sakiyama,& M Huang, *J Sound Vib,* 17 (1998) 705.

16 Liew K, & K Lim M, *J Sound Vib*, 165 (1993) 45.

17 Efraim E, & Eisenberger M, J *Sound Vib,* 299 (2007) 720.

18 Kumar V, Singh S J, Saran V H, & Harsha S P, *Eur J Mech A/Solids,* 85(2021) 104124.

19 Chakraverty S, & Pradhan K K, *Aerosp Sci Technol*, 36(2014) 132.

20 Joshan Y S, Grover N, & Singh B N, *Compos Struct*, 182 (2017)685.

21 Mizusawa T, *Int J Solids Struct,* 46 (1993) 451.